Draft version January 30, 2017
Preprint typeset using LaTeX style AASTeX6 v. 1.0

arXiv:1701.07887v1 [astro-ph.GA] 26 Jan 2017

A COMPARISON OF TWO METHODS FOR ESTIMATING BLACK HOLE SPIN IN ACTIVE GALACTIC NUCLEI

Daniel M. Capellupo[1]
Department of Physics, McGill University, Montreal, QC, H3A 2T8, Canada
McGill Space Institute, McGill University, Montreal, QC, H3A 2A7, Canada

Gaylor Wafflard-Fernandez
Department of Physics, Université Paris-Sud, Orsay, France

Daryl Haggard
Department of Physics, McGill University, Montreal, QC, H3A 2T8, Canada
McGill Space Institute, McGill University, Montreal, QC, H3A 2A7, Canada

[1]danielc@physics.mcgill.ca

ABSTRACT

Angular momentum, or spin, is a fundamental property of black holes (BHs), yet it is much more difficult to estimate than mass or accretion rate (for actively accreting systems). In recent years, high-quality X-ray observations have allowed for detailed measurements of the Fe Kα emission line, where relativistic line broadening allows constraints on the spin parameter (the X-ray reflection method). Another technique uses accretion disk models to fit the AGN continuum emission (the continuum-fitting, or CF, method). Although each technique has model-dependent uncertainties, these are the best empirical tools currently available and should be vetted in systems where both techniques can be applied. A detailed comparison of the two methods is also useful because neither method can be applied to all AGN. The X-ray reflection technique targets mostly local ($z \lesssim 0.1$) systems, while the CF method can be applied at higher redshift, up to and beyond the peak of AGN activity and growth. Here, we apply the CF method to two AGN with X-ray reflection measurements. For both the high-mass AGN, H1821+643, and the Seyfert 1, NGC 3783, we find a range in spin parameter consistent with the X-ray reflection measurements. However, the near-maximal spin favored by the reflection method for NGC 3783 is more probable if we add a disk wind to the model. Refinement of these techniques, together with improved X-ray measurements and tighter BH mass constraints, will permit this comparison in a larger sample of AGN and increase our confidence in these spin estimation techniques.

Keywords: accretion, accretion disks — black hole physics — galaxies: active — galaxies: Seyfert

1. INTRODUCTION

Actively accreting black holes have three fundamental properties – mass (M_{BH}), accretion rate ($\dot{M}$), and angular momentum. Measuring M_{BH} for active galactic nuclei at all redshifts has become possible due to reverberation mapping of low-redshift AGN and the extrapolation of those results to high redshifts, via relations between M_{BH} and the widths of broad emission lines and the AGN continuum luminosity. Accretion rate estimates have also been achieved for many AGN, usually via the Eddington ratio, L/L_{Edd}.

The angular momentum, or spin (a_*), of active BHs is more elusive, as it requires probing the region near the inner edge of the accretion disk (AD). Yet measurements of spin and spin evolution would provide valuable clues to the accretion history of active BHs and perhaps the evolution of the AGN and host galaxies themselves.

At present, there are two primary methods for constraining the spin parameters of actively accreting BHs: (1) measuring the Fe Kα emission line and/or a soft X-ray excess that some attribute to relativistic reflection (e.g. Brenneman 2013; Reynolds 2014), and (2) fitting the AGN continuum emission (CF) (e.g. Done et

al. 2013; Capellupo et al. 2016). There are significant advantages and drawbacks to each method.

The Fe Kα method is based on relativistic X-ray reflection. It does not require prior knowledge of M_{BH}, the distance to the source, or the inclination of the disk, whereas these are all necessary ingredients for the CF method. The main drawback, however, is that a very high-quality X-ray spectrum is required to properly model the continuum emission and the Fe-Kα emission line, severely limiting the number of sources for which current technology allows a spin measurement. As a result, most AGN with reflection measurements are at a redshift less than 0.1. Furthermore, the Fe Kα emission line is present in just $\sim$40% of bright, nearby type I AGN (de La Calle Pérez et al. 2010), so some spin estimates are based on modeling just a soft X-ray excess (e.g. Reynolds et al. 2014, hereafter, R14).

The CF method, on the other hand, can be applied to any AGN where the continuum emission can be measured. This vastly increases the number of AGN for which a spin measurement can be made and has already been applied out to a redshift of $\sim$1.5 (Capellupo et al. 2015, 2016). The primary drawback is that wide wavelength coverage, sometimes exceeding the capabilities of a single observatory, is required to properly measure the shape of the SED. Furthermore, this method cannot be applied effectively if the peak of the AD spectrum occurs in a wavelength regime inaccessible to current observatories, e.g., the extreme UV (where many AGN spectra do indeed peak). This method generally assumes a thin AD model, based on Shakura & Sunyaev (1973).

Recent work has directly cast doubt on the X-ray reflection method. Boissay et al. (2016) find that the soft X-ray excess that some attribute to relativistic reflection is more likely due to warm Comptonization. Similarly, Yaqoob et al. (2016) is able to fit the Fe Kα emission line for one of the AGN with an X-ray reflection spin measurement without invoking relativistic reflection. For the CF method, while the standard thin AD model has been successful in fitting the UV-optical SEDs of many AGN (see e.g. Capellupo et al. 2015, 2016), other work has found that the AGN SED can be fit with the combination of a thermal disk component and a warm Comptonization component (Mehdipour et al. 2011), indicating the possibility of greater complexity in the continuum emission.

With these two methods now available and actively in use for the estimation of a_* in AGN, it is time to investigate whether these two methods give consistent results when applied to the same AGN. This is especially important given the uncertainties in both techniques and because neither method can probe the full AGN population.

In this work, we compare the X-ray reflection and CF methods for two nearby AGN – H1821+643 and NGC 3783. Ours is among the first attempts to make this comparison (see also, Done & Jin 2016). Both targets have a published spin estimate from the reflection method. We perform the CF analysis and compare the results in detail. In §2, we describe how we selected sources for this study and our search for appropriate archival data. In §3, we describe the models and CF procedure (based on Capellupo et al. 2015, 2016). §4 and §5 describe our application of the CF method to the two AGN, and we conclude in §6 with a discussion of our results and how the reflection and CF method compare for these two case studies. We assume a ΛCDM model with $\Omega_\Lambda = 0.7$, $\Omega_m = 0.3$, and $H_0 = 70\,\mathrm{km\,s^{-1}\,Mpc^{-1}}$.

2. SAMPLE SELECTION AND DATA SOURCES

According to Vasudevan et al. (2016), there are currently 25 AGN with spin estimates from the X-ray reflection method. We use this list as a starting point to search for archival data to which the CF method can be applied.

The CF method is most effective when the "turnover" in the AD spectrum is probed. This turnover occurs at shorter wavelengths for smaller black hole masses. We therefore look first for existing high-quality UV spectroscopic observations of these AGN. Via the MAST web portal[1], we identify four AGN with high-level data products for Hubble Space Telescope (HST) Faint Object Spectrograph (FOS) observations (Evans & Koratkar 2004): Fairall 9, NGC 3783, NGC 4151, and H1821+643.

While the FOS spectrum is sufficient for applying the CF method for H1821+643, data at even shorter wavelengths is required for the lower–M_{BH} Seyfert galaxies. We seek quasi-simultaneous data, and, for NGC 3783, we identify observations from ROSAT – taken on 1992 July 23, just four days prior to the FOS observation on 1992 July 27 – that probe the appropriate wavelengths (Alloin et al. 1995). Hence we proceed with two objects, H1821+643 and NGC 3783, for our detailed spin comparison.

The FOS spectra for H1821+643 and NGC 3783 are focused on the nucleus of the galaxy. For H1821+643, we verify that the FOS spectrum (shown in Fig. 1) is dominated by AGN emission based on the broad-band star formation SED fit in Farrah et al. (2002). Similarly for NGC 3783, the spectrum is at short enough wavelengths that the host galaxy contribution should be negligible (Reichert et al. 1994; Alloin et al. 1995). Therefore, we do not correct the FOS spectra for stellar emission.

[1] https://archive.stsci.edu/

The only correction we make to the HST data is to divide out the Galactic extinction, using the Cardelli et al. (1989) extinction law and the Schlafly & Finkbeiner (2011) recalibration of the Schlegel et al. (1998) maps.

The ROSAT data have been analyzed (Turner et al. 1993, hereafter, T93), and we make no further corrections in this work.

3. ACCRETION DISK MODELS AND BAYESIAN ROUTINE

To apply the CF method, a model is required that can make specific predictions for the emitted radiation at each wavelength. Standard thin AD theory (Shakura & Sunyaev 1973) has been used for several decades to describe AGN continuum emission. Newer models use this framework, but incorporate general relativistic corrections, comptonization in the disk atmosphere, and even disk winds (e.g. Hubeny et al. 2001; Davis & Laor 2011; Slone & Netzer 2012). Here we adopt the numerical code described in Slone & Netzer (2012), assuming a viscosity parameter (α) of 0.1.

The shape and luminosity of the thin AD spectrum is mainly set by M_{BH}, $\dot{M}$, a_*, and the inclination of the disk to our line-of-sight. If we want to constrain a_*, prior knowledge of the other parameters is necessary as the observed SED is not enough to break the parameter degeneracy of the models, where different combinations of these parameters can yield similar SED shapes. Additionally, any intrinsic reddening in the AGN host galaxy will affect the observed SED shape.

We therefore adopt a Bayesian approach that takes a large grid of models – with varying values of M_{BH}, $\dot{M}$, a_*, inclination, and reddening – and maximizes the probability that any given model is a good representation of the data, while penalizing those models that are not consistent with the priors, which we establish for M_{BH} and $\dot{M}$ (Capellupo et al. 2015, 2016). This routine calculates a χ^2 value for each model, using continuum windows along the observed SED.

For the prior on M_{BH}, the reverberation mapping technique has been used to obtain M_{BH} for nearby AGN (e.g., Peterson et al. 2004), and these results have been extended to other AGN, using the width of the broad emission lines and the continuum luminosity (the 'single-epoch method'; e.g., Bentz et al. 2009; Mejía-Restrepo et al. 2016). A prior on $\dot{M}$ can be estimated using M_{BH} and a measurement of the continuum luminosity at longer (i.e., optical or near-infrared) wavelengths, assuming the canonical power law, $L_\nu \propto \nu^{1/3}$ (Collin et al. 2002; Davis & Laor 2011; Netzer & Trakhtenbrot 2014).

For the disk inclination, the only constraint we have is that our sample contains type-1 AGN, so we can consider only inclinations where $\cos\,\theta > 0.5$. For intrinsic reddening, to limit the number of free parameters, we use a simple power-law curve, where $A(\lambda) = A_o\lambda^{-1}$ mag. We consider values of A_V ranging from 0.0 to 0.50 mag.

4. H1821+643

H1821+643 is a brightest cluster galaxy (BCG) hosting a luminous AGN at $z \sim 0.297$. There are no direct reverberation mapping measurements for H1821+643, but there have been several attempts to obtain M_{BH} via other methods. These estimates range from $\sim$1.2 to $6 \times 10^9 M_\odot$ (Decarli et al. 2008; Dasyra et al. 2011; R14), and there are theoretical arguments that the mass could be as high as 3×10^{10} $M_\odot$ (Walker et al. 2014). We adopt the most recent 'single-epoch' measurement using the Hβ emission line, $M_{BH} = 2.5 \times 10^9 M_\odot$, from Decarli et al. (2008), and we use their measurement of $\log\,\lambda L_\lambda(5100\text{Å}) = 46.1$ ergs s^{-1} for calculating $\dot{M}$. We adopt errors of 0.3 and 0.2 dex, respectively, for M_{BH} and $\dot{M}$ (Capellupo et al. 2015).

Table 1. Model Parameters and Results

Object	$\log M_{BH}^{obs}$ ($M_\odot$)	$\log \dot{M}^{obs}$ ($M_\odot$ yr^{-1})	L/L_{Edd}	$\cos\,\theta$	A_V (mag)	a_*^{CF}	a_*^{ref}
H1821+643	9.4	0.48	$0.14^{+1.8}_{-0.11}$	$0.85^{+0.15}_{-0.09}$	$0.12^{+0.15}_{-0.12}$	$0.5^{+0.5}_{-0.4}$	≥ 0.40[a]
NGC 3783	7.47	-1.9	$0.020^{+0.096}_{-0.014}$	$0.89^{+0.11}_{-0.09}$	$0.17^{+0.11}_{-0.09}$	$0.2^{+0.7}_{-0.9}$	≥ 0.88[b]
NGC 3783[c]	7.47	-1.9	$0.032^{+0.15}_{-0.018}$	$0.90^{+0.10}_{-0.09}$	$0.09^{+0.09}_{-0.06}$	$0.5^{+0.5}_{-0.4}$	

[a] R14

[b] B11

[c] CF with disc wind

The best-fit (i.e., the most probable) model is presented in Fig. 1, and the full results are shown as prob-

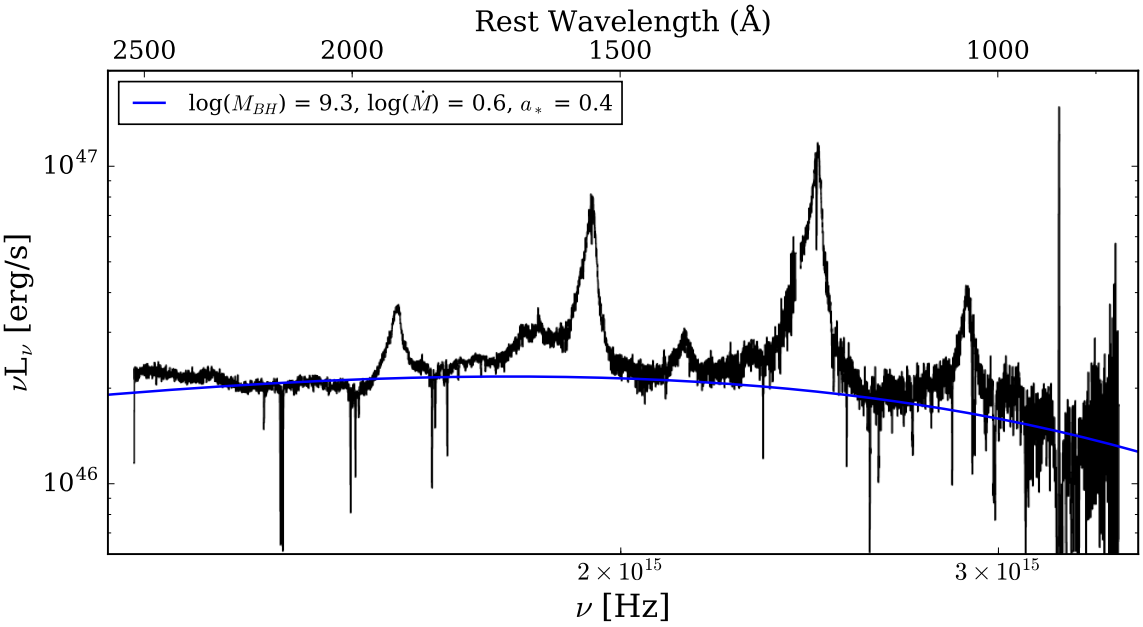

Figure 1. The HST FOS spectrum (black curve) of H1821+643, with no intrinsic reddening correction. The best-fit CF model is overplotted.

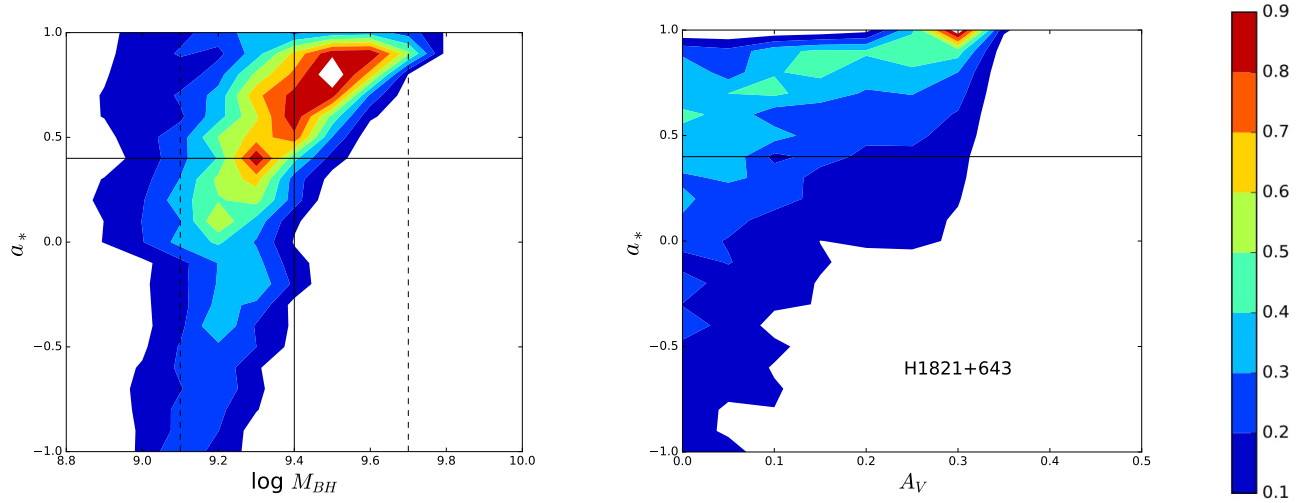

Figure 2. Posterior probability contour plots for H1821+643 for a_* versus M_{BH} and a_* versus A_V. The vertical lines identify the observed M_{BH} and the 0.3 dex error. The horizontal line identifies the lower limit on a_* from R14.

ability contours in Fig. 2. From Fig. 2, it is clear that there is a strong preference for a large, positive spin parameter.

In their analysis of the X-ray spectrum of H1821+643, R14 obtain both a constraint on the spin parameter and a constraint on L/L_{Edd} and the inclination. Applying these constraints to our CF routine, we obtain a similar probability distribution along the spin parameter axis as we did originally without these constraints.

5. NGC 3783

NGC 3783 is a well-studied Seyfert 1, SBa galaxy at $z \sim 0.009$. The reverberation mapping technique has been applied to NGC 3783, giving $M_{BH} = 2.98 \pm 0.54 \times 10^7\ M_\odot$, with a corresponding continuum luminosity, log $\lambda L_\lambda(5100\text{Å}) = 43.26 \pm 0.04$ ergs s^{-1}, which we use to estimate $\dot{M}$.

Because NGC 3783 is in a lower M_{BH} regime than H1821+643, the peak of the AD emission is in the extreme UV, a regime where we generally lack observations. We can discriminate between different spin parameters only in the soft X-ray, where models with the

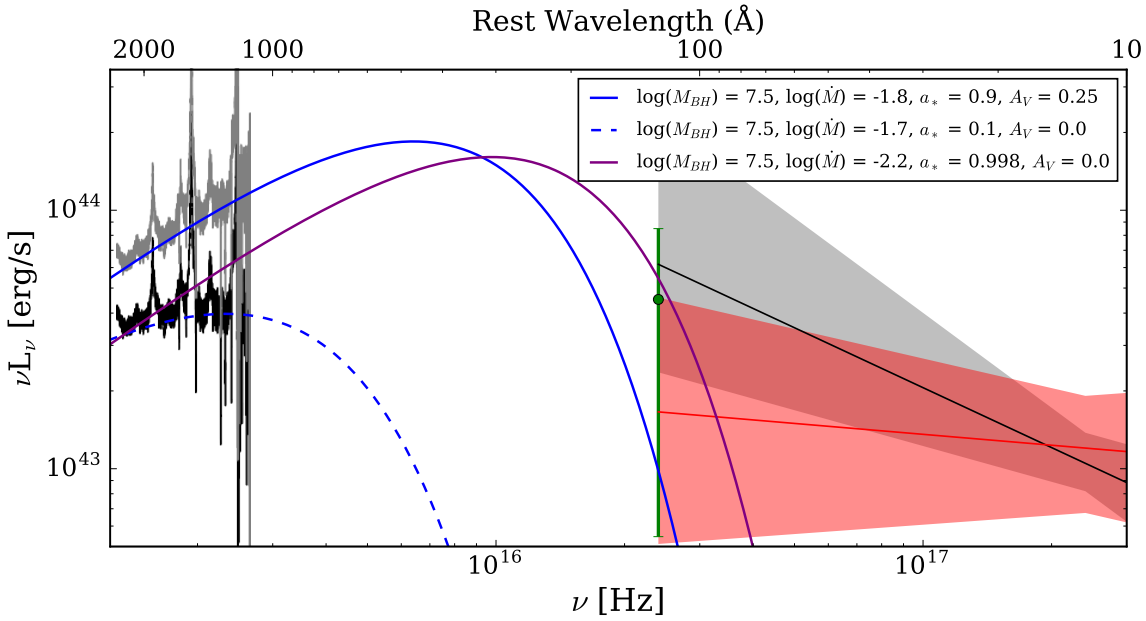

Figure 3. The FOS spectrum (black curve) of NGC 3783, corrected for intrinsic reddening (gray curve), and the ROSAT (black) and EXOSAT (red) power-laws from T93, with shaded regions denoting the 1σ error intervals. The solid and dashed blue curves are the best-fit models without and with a disk wind, respectively.

highest spin parameters peak for lower-mass BHs.

NGC 3783 has a complex X-ray spectrum, with warm absorbers and a soft excess that appears and disappears (Netzer et al. 2003). We use ROSAT X-ray data (see §2), in addition to the FOS data, to apply the CF method to NGC 3783. We use the 1992 July 23 ROSAT observation, in particular, because it is nearly contemporaneous with the FOS observation, and it extends to slightly lower energy (down to 0.1 keV) than more recent X-ray observations with Chandra or XMM Newton. T93 fits the ROSAT data with several different power-laws based on different absorption models, ranging from a simple power-law model with $\Gamma = 2.22$ to a warm absorber model with $\Gamma = 2.77^{+0.45}_{-0.31}$ (which is similar to the value found by Schartel et al. 1997 of $\Gamma = 2.7 \pm 0.7$). T93 also present a model with $\Gamma \sim 4.7$, which is much higher than other values in the literature, so we do not include it in our analysis.

5.1. *Applying the CF Method with an X-ray Upper-limit*

A difficulty with using the X-ray spectrum of an AGN for the CF method is that there is a known power-law component at X-ray wavelengths of unknown origin, in addition to possible emission from the AD. Hence, the X-ray data provides only an upper limit on the AD emission.

We therefore first alter our CF method to search through our model parameter space for the models with the highest spin parameter that give both a satisfactory fit to the FOS spectrum ($\chi^2 \leq 3$) and do not exceed the X-ray flux at 0.1 keV from the power-law fits to the ROSAT data. To be conservative in our upper limit, we adopt the warm absorber model power law ($\Gamma = 2.77^{+0.45}_{-0.31}$) from T93.

We find models spanning the full range in spin parameter, including maximum spin, that can fit within the upper limit from the T93 warm absorber model power-law for the ROSAT data, as long as M_{BH} is at least as high as the Peterson et al. (2004) M_{BH} estimate (see, for example, the purple curve in Fig. 3).

5.2. *Applying the CF Method with a Modified X-ray Flux*

Even for a maximally spinning black hole, the thin AD emission does not directly contribute to the hard X-ray band (i.e., above 2 keV; see Fig. 3). Hard X-ray observations of NGC 3783 give a less steep power law than in the soft X-ray band. For example, T93 find $\Gamma = 2.14^{+0.24}_{-0.26}$ when applying their warm absorber model to data from EXOSAT. If we assume that the excess emission indicated by a steeper powerlaw in the soft X-ray band is due to AD emission, we can subtract the hard X-ray powerlaw from the soft powerlaw at 0.1 keV to determine a continuum point for our regular Bayesian CF procedure.

We use a value of 0.1 dex for the error on M_{BH} from Peterson et al. (2004). The results of the CF routine are presented in the left panel of Fig. 4, and we find a median $a_* \simeq 0.2^{+0.7}_{-0.9}$. Using the X-ray reflection method, Brenneman et al. (2011, hereafter B11) determine a spin parameter $a_* \geq 0.98$ at 90% confidence and $a_* \geq 0.88$

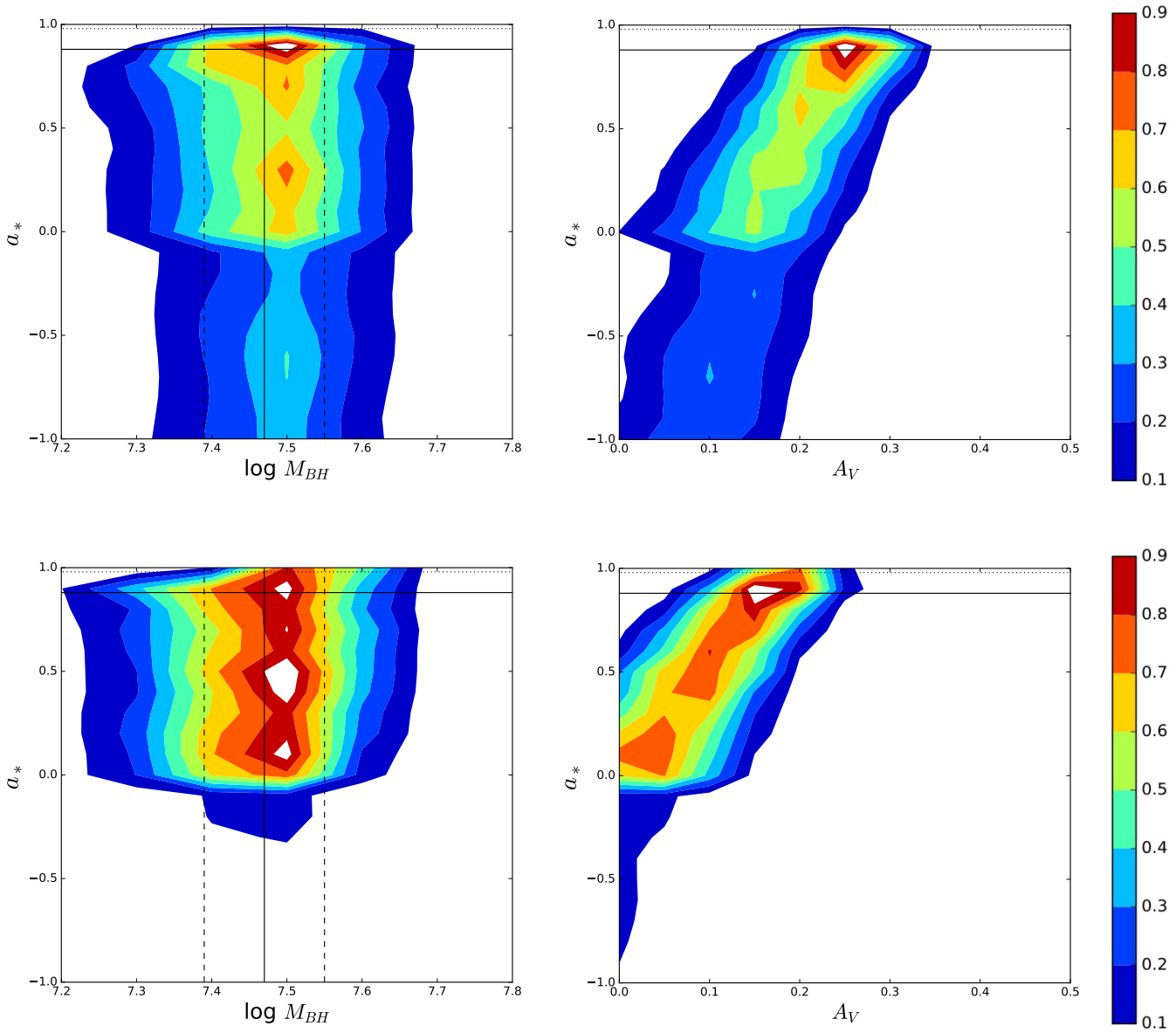

Figure 4. Probability contour plots for NGC 3783 for a_* versus M_{BH} (left panels) and a_* versus A_V (right panels) for two different iterations of the Bayesian CF routine: without a disc wind (top panels) and with a disc wind (bottom panels). The observed value of M_{BH} and associated error is indicated by vertical solid and dashed lines, respectively. The horizontal dotted and solid lines represent the 90% and 99% confidence on a_* from B11.

at 99% confidence (indicated by horizontal dotted and solid lines in Fig. 4).

5.3. *Applying the CF Method with an AD Wind*

NGC 3783 is known to have a warm absorber in its X-ray spectrum (T93), i.e. an outflow often presumed to originate from the AD of the AGN (e.g., Tombesi et al. 2013). If this is the case for NGC 3783, then the thin AD model must be modified, as the accretion rate would be reduced throughout the disk as material is ejected.

The Slone & Netzer (2012) thin AD code provides the option of adding a disk wind to the model. We therefore rerun the CF routine using a model with a self-similar disk wind, where the mass outflow rate per decade of radius is constant. The mass outflow rate for NGC 3783 has been estimated to be $\gtrsim 160$ times the accretion rate; however, much of this outflowing gas may come from beyond the accretion disk (T93; Crenshaw & Kraemer 2012). In the absence of an empirical estimate of the mass outflow rate from the disk itself, we illustrate the affect of a massive disk wind by choosing a mass accretion rate at the outer part of the disc equal to three times the accretion rate at the innermost stable circular orbit (ISCO). The results are presented in the right

panel of Fig. 4.

The main difference between these results and the results without the disk wind is that lower spin parameters ($a_* < 0$) are much less probable in the disk wind scenario. This arises because the disk wind reduces the accretion rate in the inner part of the disk and thus suppresses the luminosity at short wavelengths. Furthermore, while there is a high probability of $a_* \geq 0.88$ both with and without a disk wind, there is clearly a lower probability of having $a_* \geq 0.98$ if there is no disk wind (there is a factor of $\sim$1.6 difference in radiative efficiency between these two spin parameters). There is also a positive correlation between the amount of intrinsic reddening and a_*, with $a_* \geq 0.88$ ruled out if there is close to zero reddening.

6. DISCUSSION

Our aim in this work is to compare the derived spin parameters for the X-ray reflection and CF techniques for two "case study" AGN. Table 1 summarizes the results of the two methods, including values for L/L_{Edd}, the disk inclination (θ), and instrinsic reddening, as derived from the CF method.

For H1821+643, a bright AGN with $M_{BH} \sim 2.5 \times 10^9 M_\odot$, R14 found $a_* \gtrsim 0.4$ using the reflection method. For the CF analysis, the HST FOS spectrum alone is sufficient, and while we do not obtain a very precise constraint on a_*, we find a strong probability of a spin parameter that exceeds the lower limit from R14, giving consistent results between the reflection and the CF method. We emphasize here that R14 do not clearly detect an Fe line, but instead fit excess continuum emission in the soft X-ray. For some AGN, physical processes other than relativistic reflection are the more likely cause of this soft excess (Boissay et al. 2016, and references therein), making this reflection spin measurement a tentative one (see also §1). For the CF method, from the posterior probability distribution, it is clear that if M_{BH} is higher, then a_* would be constrained to the highest allowed values. Whereas, if M_{BH} is any lower, we would be unable to obtain a meaningful constraint on a_*.

For NGC 3783, the FOS spectrum lies along the power-law portion of the thin AD model spectrum, and only in the soft X-ray regime can models with different a_* be distinguished. Fortunately, there is nearly contemporaneous FOS and ROSAT data for NGC 3783. However, the X-ray data includes the known X-ray power-law emission that likely originates from above the AD (often called the "corona"). Using the X-ray flux as an upper-limit, we find that as long as M_{BH} is at least as high as the observed M_{BH}, any spin parameter could fit the data.

Since there are other components besides the AD emission in the X-ray, if we assume that just the excess emission indicated by the steeper powerlaw slope in the soft X-ray, compared to in the hard X-ray, is due to the AD itself, applying the CF method to NGC 3783 gives a high probability for a high spin parameter, consistent with the 99% confidence lower limit from relativistic reflection (B11). However, there is a low probability of a_* exceeding the 90% confidence lower limit from B11, unless we include a disk wind in the AD model.

The results of the CF method are, in general, consistent with the results of the reflection method for the two AGN studied here. In particular, the agreement is improved for NGC 3783 if we assume a disc wind, which we include based on the existence of a warm absorber in the X-ray spectrum. The disk wind analysis, however, is tentative because it is unknown how much, if any, of the outflow originates from the inner part of the disk (see e.g. Netzer et al. 2003). If the outflow originates further out and therefore does not suppress the short wavelength thin AD emission, there is a slight tension between the two methods, as the reflection method suggests a slightly higher spin parameter than the CF method without a disk wind. We also find that, without a disc wind, the highest spins are most probable for A_V between 0.2 and 0.3 mag. While these reddening values are generally consistent with the constraints from broad emmission line measurements for NGC 3783 (A_V=0.1$\pm$0.2; Schnorr-Müller et al. 2016), if the reddening is actually closer to 0.1 mag, then there is even greater tension between the reflection and CF results for a_*. Done et al. (2013) and Done & Jin (2016) similarly find that the CF method suggests lower spin parameters for narrow-line Seyfert 1s than the nearly maximal spin typically found for this AGN subclass via X-ray reflection.

Our study highlights one particular strength of the X-ray reflection method for nearby Seyfert galaxies. For NGC 3783, with a BH mass of $\sim 10^7$ $M_\odot$, the inability to probe the extreme UV prevents us from obtaining a very precise estimate of a_*. However, we point out that recent work by Yaqoob et al. (2016) casts doubt on whether the Fe Kα line gives any information on a_* for one of the AGN in the reflection sample (see also §1).

Nearly half (12) of the 25 AGN with spin measurements from the reflection method have $a_* > 0.9$ (Vasudevan et al. 2016). Given that the CF method suggests lower spin for two cases with near-maximal reflection spin estimates (1H 0707$-$495 in Done & Jin 2016 and NGC 3783 presented here), these high-spin cases would be good candidates for further comparisons between the reflection and CF methods, especially those with even lower M_{BH} than NGC 3783, whose AD SEDs would peak further into the soft X-ray. There is also a new method proposed by Chartas et al. (2016), based on microlensing, that could be included in future com-

parisons of spin estimation techniques.

As more and better X-ray measurements allow the reflection sample to grow and as better constraints on M_{BH} (see e.g., Shen et al. 2015; Mejía-Restrepo et al. 2016) allow the CF method to more precisely determine a_* for larger samples of AGN, there will be a larger population where both methods can be properly applied and compared. If such comparisons yield good agreement, then each method can be more confidently applied to the samples they are best suited for – nearby Seyferts for the X-ray reflection method and higher redshift quasars for the CF method. If instead, these comparisons bring further tensions to light, then the assumptions underlying these methods may need to be revisited.

We thank the referee for helpful feedback. We thank Paulina Lira, Julie Hlavacek-Larrondo, and Helen Russell for useful discussion. DMC and DH acknowledge support from a Natural Sciences and Engineering Research Council of Canada Discovery Grant and a Fonds de recherche du Québec Nature et Technologies Nouveaux Chercheurs Grant. GWF acknowledges support from Université Paris-Saclay's IDEX program and l'Office Franco-Québécois pour la Jeunesse.

REFERENCES

Alloin, D., Santos-Lleo, M., Peterson, B. M., et al. 1995, A&A, 293
Bentz, M. C., Walsh, J. L., Barth, A. J., & et al. 2009, ApJ, 705, 199
Boissay, R., Ricci, C., & Paltani, S. 2016, A&A, 588, A70
Brenneman, L. 2013, Measuring the Angular Momentum of Supermassive Black Holes, SpringerBriefs in Astronomy. ISBN 978-1-4614-7770-9. Laura Brenneman, 2013,
Brenneman, L. W., Reynolds, C. S., Nowak, M. A., et al. 2011, ApJ, 736, 103
Capellupo, D. M., Netzer, H., Lira, P., Trakhtenbrot, B., & Mejía-Restrepo, J. 2015, MNRAS, 446, 3427
—. 2016, MNRAS, 460, 212
Cardelli, J. A., Clayton, G. C., & Mathis, J. S. 1989, ApJ, 345, 245
Chartas, G., Krawczynski, H., Zalesky, L., et al. 2016, arXiv:1609.09490
Collin, S., Boisson, C., Mouchet, M., et al. 2002, A&A, 388, 771
Crenshaw, D. M., & Kraemer, S. B. 2012, ApJ, 753, 75
Dasyra, K. M., Ho, L. C., Netzer, H., et al. 2011, ApJ, 740, 94
Davis, S. W., & Laor, A. 2011, ApJ, 728, 98
de La Calle Pérez, I., Longinotti, A. L., Guainazzi, M., et al. 2010, A&A, 524, A50
Decarli, R., Labita, M., Treves, A., & Falomo, R. 2008, MNRAS, 387, 1237
Done, C., & Jin, C. 2016, MNRAS, 460, 1716
Done, C., Jin, C., Middleton, M., & Ward, M. 2013, MNRAS, 434, 1955
Evans, I. N., & Koratkar, A. P. 2004, ApJS, 150, 73
Farrah, D., Serjeant, S., Efstathiou, A., Rowan-Robinson, M., & Verma, A. 2002, MNRAS, 335, 1163
Hubeny, I., Blaes, O., Krolik, J. H., & Agol, E. 2001, ApJ, 559, 680
Mehdipour, M., Branduardi-Raymont, G., Kaastra, J. S., et al. 2011, A&A, 534, A39
Mejía-Restrepo, J. E., Trakhtenbrot, B., Lira, P., Netzer, H., & Capellupo, D. M. 2016, MNRAS, 460, 187
Netzer, H., & Trakhtenbrot, B. 2014, MNRAS, 438, 672
Netzer, H., Kaspi, S., Behar, E., et al. 2003, ApJ, 599, 933
Peterson, B. M., Ferrarese, L., Gilbert, K. M., et al. 2004, ApJ, 613, 682
Reichert, G. A., Rodriguez-Pascual, P. M., Alloin, D., et al. 1994, ApJ, 425, 582
Reis, R. C., Reynolds, M. T., Miller, J. M., & Walton, D. J. 2014, Nature, 507, 207
Reynolds, C. S. 2014, SSRv, 183, 277
Reynolds, C. S., Lohfink, A. M., Babul, A., et al. 2014, ApJL, 792, L41
Schartel, N., Schmidt, M., Fink, H. H., Hasinger, G., & Truemper, J. 1997, A&A, 320, 696
Schlafly, E. F., & Finkbeiner, D. P. 2011, ApJ, 737, 103
Schlegel, D. J., Finkbeiner, D. P., & Davis, M. 1998, ApJ, 500, 525
Schnorr-Müller, A., Davies, R. I., Korista, K. T., et al. 2016, MNRAS, 462, 3570
Shakura, N. I., & Sunyaev, R. A. 1973, A&A, 24, 337
Shen, Y., Brandt, W. N., Dawson, K. S., et al. 2015, ApJS, 216, 4
Slone, O., & Netzer, H. 2012, MNRAS, 426, 656
Tombesi, F., Cappi, M., Reeves, J. N., et al. 2013, MNRAS, 430, 1102
Turner, T. J., Nandra, K., George, I. M., Fabian, A. C., & Pounds, K. A. 1993, ApJ, 419, 127
Vasudevan, R. V., Fabian, A. C., Reynolds, C. S., et al. 2016, MNRAS, 458, 2012
Walker, S. A., Fabian, A. C., Russell, H. R., & Sanders, J. S. 2014, MNRAS, 442, 2809
Yaqoob, T., Turner, T. J., Tatum, M. M., Trevor, M., & Scholtes, A. 2016, MNRAS, 462, 4038